Beta dose attenuation in thin layers

Rainer Grün
Department of Geology
McMaster University
1280 Main Street West
Hamilton, Ontario
Canada L8S 4M1

In attempting to date tooth enamel or thin mollusc shells by ESR or TL the beta-ray contribution from the surroundings may be the decisive factor in calculating the annual dose. Normally, the alpha-ray penetrated surface (up to 20µm) of a sample can be removed by etching or by means of a dentist's diamond drill. The gamma-ray contribution can be measured by TLD's or calibrated portable gamma spectrometers (Murray, 1981; Grün, 1985). The beta-ray contribution is, however, more difficult to estimate because the range of the beta particles is comparable to the thickness of the shell or enamel layer. In order to solve this problem, average beta dose curves were calculated according to modified formulas given by Yokoyama et al. (1982).

A beta particle with maximun energy E (Mev) has an effective beta-range P (in cm) into a sample with density ρ (in g/cm^3):

$$P = 0.0825\ [(1 + 22.4\ E^2)^{0.5} - 1]\ /\rho \qquad (1)$$

The average dose D received by a volume of thickness d cm subjected to a beta source with infinite matrix dose D_0 can be calculated by the following formula (assuming that the sample is irradiated from one side only (2π-geometry)):

$$D = [0.5\ D_0\ /\ \mu d]\ [1 - \exp(-\mu d)] \qquad (2)$$

where μ is the linear attenuation coefficient per cm ($\mu = 3.3\ /\ P$).

The average dose for a sample with total thickness d cm from which a surface layer of x cm has been removed can be calulated by (see also Aitken et al., 1985):

$$D_{(d-x)} = [0.5\ D_0 / \mu\ (d-x)]\ [\exp(-\mu x) - \exp(-\mu d)] \qquad (3)$$

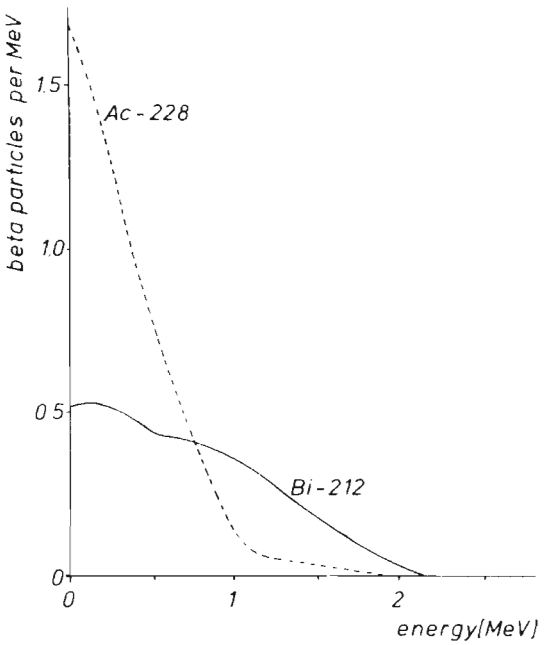

Figure 1: Beta spectra for Ac-228 and Bi-212 (Cross, pers. comm.).

In a β^- decay a negative electron (beta particle) and a neutrino are emitted from the nucleus. The released energy is divided statistically between the beta-particle and the neutrino. When observing a large number of transitions, the beta particle and the neutrino both have energy distributions ranging from zero to the maximum energy available, E_{max}. A beta transition to a particular energy level is characterized by E_{max} and the average energy, E_{av}, of the emitted beta particles. Within the beta decay from a parent to a daughter isotope various transitions with definite probabilities may occur. These processes produce characteristic beta spectra for each beta emitter as e.g. shown in Fig. 1 (Cross, pers. comm.). The spectra of Ac-228 and Bi-212 have about the same maximum energy (2.089 and 2.246, resp.), but very different shapes. These shapes reflect the E_{max} values of the constituent transitions; for instance, in the case of Ac-228 there are ten principal transitions with E_{max} values of 2.08, 1.82, 1.75, 1.18, 1.13, 1.03, 1.0, 0.62, 0.49, and 0.46 MeV, the probabilities being 6%, 2.7%, 14%, 39%, 11%, 3.5%, 7.9% 4.6%, 6.9%, and 5.3% respectively. (It may be noted that the E_{max} values given by Bell (1976) are weighted averages, the value given for Ac-228 being 1.21 MeV). Additionally, internal conversion electrons (IC) can be emitted from the nucleus as an alternative to gamma-ray emission. This process can produce a vacancy in the inner electron shell. The filling of this vacancy generates X-rays or Auger electron emission. Electron replacement of vacancies caused by the filling

of the initial vacancy can produce further Auger electrons (and X-rays).

In order to consider the characteristic beta spectra to some extent, the formulas (1) and (2) were applied to each electron transition occuring in the U- and Th-decay chains. Maximum and average beta energies have been published by Martin & Blichert-Toft (1970; K-40, Th-232 decay chain, and Ra-226 and daughters), Ellis (1977; Th-234 and Pa-234), Schmorak (1977 a&b; Th-231 and Tl-207), Maples (1977: Ac-227 and Th-227), and Martin (1978: Pb-211 and Bi-211). The energy values of the IC and Auger electrons were taken from Bell (1976, 1979). Transitions with an abundance of less than 0.1% were not considered.

In order to determine the average beta doses for a decay chain, formula (1) was applied to all transitions occurring within this chain. Formula (2) was weighted by the product of the average beta energy and the abundance of this transition, which is proportional to the dose transferred from these electrons to the sample. The sum of the latter agreed with the values given by Bell (1976) within less than 1%.

It should be kept in mind that the calculation presented here is only a first approach to this problem because, for example, the shapes of beta spectra of single transitions may vary (see Cross, 1983: spectra for K-40 and Tl-208). Baltakmens (1977) points out that the absorption coefficient of a beta emitter in Al is more likely to be proportional to the area under the curve of a beta spectrum than to its maximum or average energy. This effect cannot be considered in this attempt; it also gives evidence of the limited validity of formula (1). Mejdahl (1979) published beta attenuation data for quartz grains converting computerized beta attenuation curves of point kernels for water (Berger, 1971; 1973) to quartz using a scaling procedure developed by Cross (1968, 1982). A computer program for the planar case considered here could also be devised but would probably require about one year of effort (Prestwich, pers. comm.).

The results of the calculations are shown in Fig. 2. It is obvious that the average beta doses are considerably different for the various decay chains. Aitken et al. (1985) experimentally determined beta attenuation curves for the Th- and U-decay chains using an aluminum absorber and a wide area detector for beta TLD (see Bailiff & Aitken, 1980). They found an exponential relation between the beta dose behind the absorber and its thickness, with coefficients of 1.54 per mm (U-decay chains) and 1.78 per mm (Th-decay chain). A comparison of these results with the dose at a depth d (in cm) derived from formula (3) are shown in Fig. 3. The calculated values for the attenuation by an absorber with ρ = 2.7 g/cm^3 is higher in the first 0.1 mm than in the experiment, for both decay chains. The difference decreases with increasing thickness of the absorber up to about 1 mm, beyond which the curves diverge. The experimental attenuation curves give average beta doses (2π-geometry) for 0.1 mm thickness, which are 8.9% (U) and 18.7% (Th) higher than the calculated data. For 2.5 mm the values reach a relatively good agreement (1% (U); 6% (Th)). The experimental arrangement used by Aitken et al. (1985) was not able to detect beta rays with maximum ranges on the order of alpha-rays

(about 20 μm in solids with ρ = 2.7 g/cm^3) and the gamma component, which compensates this effect to some extent (Bailiff & Aitken, 1980), was subtracted in this experiment also for the zero-absorber dose. Therefore the experimental data cannot be compared directly with this calculation, because about 6% of the total beta dose of the U-decay chains and about 14% of the Th-decay chain are generated by beta emissions (mainly ICs), which have maximum ranges less than 20 μm. Assuming that the measured doses without absorber represent 47% and 43% of the infinite matrix dose of the U and Th source, respectively, the experimental data show good agreement with the calculated values (at 0.1 mm: 2% (U), 2% (Th); at 2.5 mm: 5% (U), 11% (Th)).

Yokoyama et al. (1982) published attenuation factors for the Th-232 decay chain, groups of emitters of the U-decay chains, and K-decay. The attenuation factor for the K-decay is the same as in the present paper since the K-decay consists of one transition only. The average beta doses applying Yokoyama's attenuation factors and relative abundances are nearly always higher (at 0.1 and 2.5 mm): Th-232 decay chain: + 10.6% and + 10%; U-238 - Th-230: + 6% and + 4%; Th-230 - Pb-206: + 5% and - 9.6%; U-235 decay chain: + 9% and + 1%. This can be explained by a different consideration of beta particles with low energies (the beta dose rates within the U-238 decay chain given by Yokoyama et al. (1982) are different to the values by Bell (1976, 1979) due to modifications for IC electrons).

When dating tooth enamel an additional effect has to be considered: an enamel lamella can be generally found within three different environments (Fig. 4):

- a single fragment of an enamel layer is embedded in sediment.
- an enamel layer lies between sediment and dentine/cement as, e.g., a broken part of a mammoth tooth-lamella.
- an enamel layer lies between dentine and cement as, e.g., in a fragment of a whole mammoth tooth.

The beta-ray contribution from the sediment can be derived from Fig. 2 assuming the decay chains to be in equilibrium. Dentine and cement, however, tend to accumulate uranium. The effect of U-uptake on ESR-age determination was discussed by Ikeya (1982) and Grün & Invernati (1985). The U-decay chain in the dentine/cement displays Th-230/U-234 disequilibrium. Fig. 5 shows that the integral beta doses produced by beta emitters from U-238 to Pb-206. Hence, when the Th-230/U-234 disequilibrium has to be considered in the dose calculation, the different beta-correction factors also have to be taken into account.

Table 1 gives the average beta doses for samples, which are irradiated from one side (as percentage of the infinite matrix dose) for the Th-232 and U-235 decay chains, the K-40 decay; for the U-238 decay chain the average doses were calculated for the beta decays above and below Th-230. The calculations were carried out for densities of 2.95 g/cm^3 (aragonite/hydroxyapatite) and 2.7 g/cm^3 (calcite). This table can be used when calculating the average beta dose of thin samples. Above 3 mm (ρ = 2·7 g/cm^3) the external beta radiation is negligible and, hence, the average beta dose can be calculated by linear extrapolation.

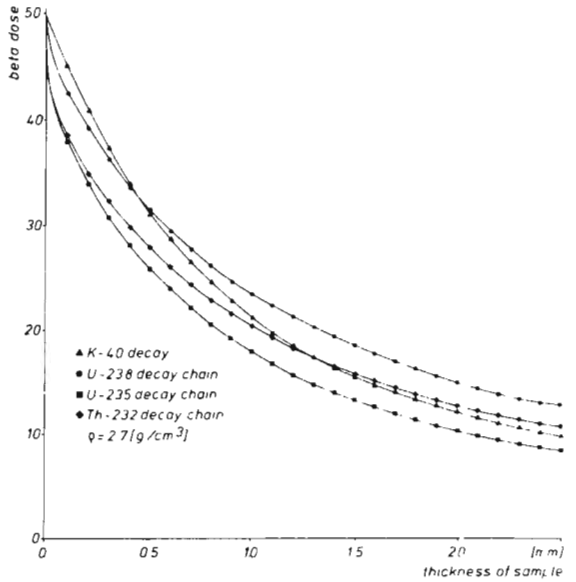

Figure 2: Average beta doses in samples, which are irradiated from one side (2π-geometry), as a percentage of the infinite matrix dose.

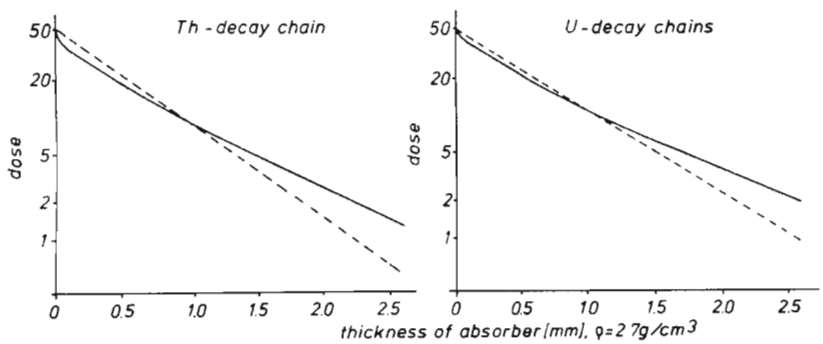

Figure 3: Comparison of the dose at depth d as derived from formula (3) (solid line) with the experimental lines as determined by Aitken et al. (1985) (dotted lines).

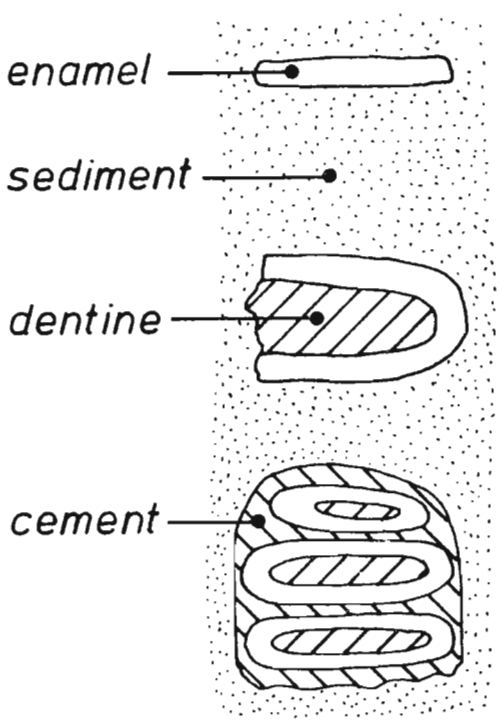

Figure 4: Possible environments of an enamel layer.

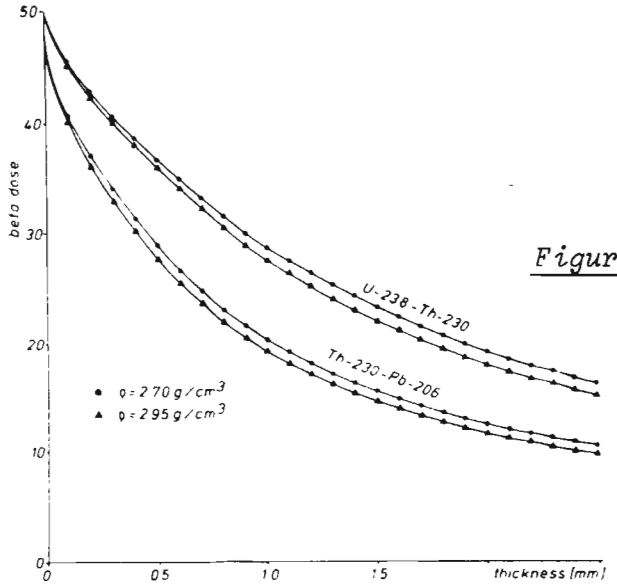

Figure 5: Average beta doses in samples (2π-geometry) for the beta decays between U-238 - Th-230 and Th-230 - Pb-206 as percentage of the infinite matrix dose.

Table 1 Average beta doses (as percentage of the infinite matrix dose) for samples with densities of 2.70 g/cm^3 (a) and 2.95 g/cm^3 (b) irradiated from one side (2π-geometry) and infinite matrix doses (imd) for 1ppm U and Th and 1% K (Bell, 1976; 1979).

Average beta dose (as percentage of the infinte matrix dose)										
	Th-232		U-238 - Th-230		Th-230 - Pb-206		U-235		K-40	
imd [mrad/a]:	2.90		5.49		8.81		0.34		83.0	
Thickness (mm)	a	b	a	b	a	b	a	b	a	b
0.02	42.8	42.6	48.7	48.6	44.8	44.7	43.2	43.0	49.0	48.9
0.05	40.3	40.6	47.4	47.2	43.1	42.9	40.6	40.3	47.5	47.3
0.1	38.6	38.2	45.6	45.3	40.8	40.4	37.9	37.5	45.2	44.8
0.2	35.1	34.5	42.9	42.5	37.0	36.3	34.0	33.3	41.1	40.3
0.3	32.3	31.6	40.6	40.0	33.7	32.9	30.9	30.1	37.4	36.5
0.4	29.9	29.1	38.5	37.8	31.0	30.0	28.2	27.4	34.2	33.0
0.5	27.9	27.0	27.3	35.7	28.6	27.6	26.0	25.0	31.4	30.2
0.6	26.4	25.1	34.8	33.9	26.5	25.4	23.9	22.9	28.8	27.6
0.8	23.0	22.0	31.6	30.5	23.0	22.0	20.6	19.5	24.7	23.3
1.0	20.5	19.5	28.8	27.6	20.3	19.3	17.9	16.9	21.3	20.0
1.2	18.4	17.4	26.4	25.1	18.1	17.1	15.7	14.7	18.7	17.4
1.4	16.6	15.7	24.2	23.0	16.4	15.4	14.0	13.0	16.5	15.3
1.6	15.2	14.2	22.3	21.1	14.9	13.9	12.5	11.6	14.7	13.6
2.0	12.8	11.9	19.2	18.0	12.5	11.7	10.3	9.5	12.1	11.1
2.5	10.6	9.8	16.2	15.0	10.5	9.7	8.3	7.7	9.8	8.9
3.0	9.0	8.3	13.9	12.8	8.9	8.3	7.0	6.4	8.2	7.5

It is hoped that in the near future a more complex calculation similar to the one performed by Mejdahl (1979) will be carried out. It has to be mentioned that even these calculations will exhibit some uncertainties since the calculations of beta-dose distributions performed by Berger (1971) show deviations of up to 6% from the values calculated by Cross et al. (1982). However, most of the thin samples investigated by ESR have rough and irregular shaped surfaces and , hence, it is difficult to determine the beta ray contribution with a good accuracy in any case. It should be noted that in a real case backscattering effects due to change of medium may be significant (see Baltakmens, 1975).

Acknowledgement

I wish to thank Dr. M.J. Aitken for providing his preprint and Dr. W.G. Cross for the beta spectra. Thanks are due to Dr. W. Prestwich for valuable comments and Dr. H.P. Schwarcz for his help on the manuscript. Financial support was provided by NSERC.

References

Aitken, M.J., Clark, P.A., Gaffney, C.F. and Lovborg, L. (1985). Beta and gamma gradients, Nuclear Tracks, 10, 647-654.

Bailiff, I.K. and Aitken, M.J. (1980): Use of thermoluminscence dosimetry for evaluation of internal beta dose-rate in archaeological dating. Nucl. Inst. Meth., 173, 423-429.

Baltakmens, T. (1975): Energy loss of beta particles on backscattering. Nucl. Inst. Meth., 125, 169-171.

-- (1977): Accuracy of absorption methods in the identification of beta emitters. Nucl. Inst. Meth., 142, 535-538.

Bell, W.T. (1976): The assessment of the radiation dose-rate for thermoluminescence dating. Archaeometry, 18, 107-111.

-- (1979): Thermoluminescence dating: radiation dose-rate data. Archaeometry, 21, 243-245.

Berger, M.J. (1971): Distribution of absorbed dose around sources of electrons and beta particles in water and other media.- J. Nucl. Med., Suppl., 5, 5-23, MIRD/Pamphlet No.7.

-- (1973). Improved point kernels for electron and beta-ray dosimetry. NBSIR, 73-107. National Bureau of Standards, Washington, D.C..

Cross, W.G., (1968) Variation of beta dose attenuation in different media. Phys. Med. Biol., 13, 611-618.

Cross, W.G., Ing. H., and Freedman, N. (1983) A short atlas of beta ray spectra. Phys. Med. Biol., 28, 1251-1260.

Cross, W.G., Ing, H., Freedman, N. and Mainville, J. (1982) Tables of beta-ray dose distributions in water, air and other media.- AECL, 7617, 89 p, Atomic Energy of Canada Ltd., Chalk River, Ont..

Ellis, Y.A. (1977) Nuclear data sheets for A = 234. Nucl. Data Sheets, 21, 493-548.

Grün, R. (1985) Beiträge zur ESR Datierung.- Sonderveröff. Geol. Inst. Univ. Köln, 59, 1-157.

Grün, R. and Invernati, C. (1985) Uranium accumulation in teeth and its affect on ESR dating - A detailled study on a mammoth tooth. Nucl. Tracks, 10, 869-878.

Ikeya, M. (1982) A model of linear uranium accumulation for ESR age of Heidelberg (Mauer) and Tautavel bones. Jap. J. Appl. Phys., 21, 690-692.

Maples, C. (1977) Nuclear data sheets for A = 227. Nucl. Data Sheets, 22, 275-323.

Martin, M.J. (1978) Nuclear data sheets for A = 211. Nucl. Data Sheets, 25. 397-432.

Martin, M.J. and Blichert-Toft, P.H. (1970) Radioactive Atoms - Auger-Electron, α-, β-, γ- and X-Ray Data. Nuclear Data Tables, A8, 1-198.

Mejdahl, V. (1979) Themoluminescence dating: Beta-dose attenuation in quartz grains. Archaeometry, 21, 61-72.

Murray, A.S. (1981) Environmental radioactivity studies relevant to thermoluminescence dating. Unpublished D.Phil. Thesis Oxford University.

Schmorak, M.R. (1977a) Nuclear data sheets for A = 231, 235, 239. Nucl. Data Sheets, 21, 91-200.

-- (1977b) Nuclear data sheets for A = 207. Nucl. Data Sheets, 22, 487-544.

Yokoyama, Y., Nguyen, H.V., Quaegebeur, J.P. and Poupeau, G. (1982) Some problems encountered in the evaluation of annual dose rate in the electron spin resonance dating of fossil bones. PACT J., 6, 103-115.

P.R. **Reviewer's Comments (MJA)**

Its satisfying to find that values for beta attenuation coefficient measured by Chris Gaffney (Aitken et al., 1985) are in reasonable agreement with prediction, and this gives confidence in utilising Table 1 (which is presumed to be for the case of x = 0 in equation (3)). The prediction is ultimately based on the empirical equation given by Flammersfield (1946, Naturwissenschaft 33 p. 280); a slightly more recent, slightly more simple equation has been given by Katz and Penfold (1952, Revs.Mod.Phys. 24 p. 28); there may be others. Readers concerned with beta attenuation may find it useful to refer to p. 628 of Evans (1955, The Atomic Nucleus, McGraw Hill).

SPECIAL NOTICE

Some paperback copies of my book TL Dating have a faulty binding. I am highly embarrassed by this and so are the publishers. If your copy is faulty you may obtain a replacement by writing to

Dr. Conrad Guettler
Academic Press
24-28 Oval Road
London
NW1 7DX

M.J. Aitken

A high performance TL disc

R. Templer
Research Laboratory for Archaeology
6 Keble Road
Oxford OX1 3QJ

The TL disc described here was the result of a search for suitable material to use in the auto-regenerative dating of zircons (Sutton and Zimmerman. 1979). Experimental criteria demanded that the disc material should exhibit no spurious, have high thermal conductivity, low emissivity, high reflectivity and mechanical toughness.

I have found that the use of rhodium plated copper provides the optimum choice. Copper discs 9.7mm in diameter and 0.020" thick are electro-plated first with an undercoat of silver and then a thin (1 micrometre) coating of rhodium. Rhodium does not oxidize and, as one would therefore expect, exhibits no detectable spurious TL. The spurious caused by leaving a disc left in air for 1 month is lost in the photomultiplier noise, which for my system means the spurious is less than 0.3cps from room temperature up to 400°C. Because of the thinness of the rhodium/silver coating, most of the disc's thermal conductivity comes from the copper (k=400 $Wm^{-1}K^{-1}$). The emissivity of rhodium is very low (ε=0.2 at 650nm and 1400 K). In the range 350 to 550nm the average reflectance of rhodium is 80%. Rhodium is also one of the most durable metals; no cracks or scratches have developed in discs either through repeated cleaning or because of the relative thermal expansion of the copper and rhodium during heating.

By comparison, the properties of other low spurious materials fall short of these discs in one or more respects. The discs can be plated by Twickenham Plating of 6 Colne Road, Twickenham, Middlesex, at a cost of 40 pence per disc.

Reference

Sutton S.R., and Zimmerman D.W. (1979) The zircon natural method: initial results and low level TL measurement. PACT J., 3, 465.

P.I. Reviewed by the Editor.

Post wash effects in zircon

Scott Wheeler
Research Laboratory for Archaeology
6 Keble Road
Oxford OX1 3QJ

Introduction

In investigating the phosphorescence associated with the anomalous fading of high temperature TL in zircon, it is necessary to use a thermal wash to eliminate interference due to phosphorescence from the low temperature peaks. This thermal pretreatment has revealed two new phenomena: a short term phosphorescence not associated with the anomalous fading and a peak at 175°C whose peak area increases with time after washing.

Post wash phosphoresence

The following experiments were performed on a coarse grain sample (ref 210R2) from the Puy de Dome (courtesy of D. Miallier), mounted in a gold pan and secured with Viscasil, and a fine grain preparation of beach sand from Kerala in India (ref 210f1), mounted on a stainless steel disc. The phenomenon has been observed in several other samples of zircon, and in one sample of quartz (not necessarily pure) extracted from pottery. In no case has a sample been found not to exhibit the phenomenon.

Discovery: The sample 210R2 was irradiated (5000Gy) and left at room temperature for 30 days to eliminate any phosphorescence from the anomalously fading component of TL (Templer, 1985). The total number of TL counts to be expected from this sample was 6×10^8. Prior to giving the sample a thermal wash, the count rate was 450cps, presumed to be thermal phosphorescence. Various thermal washes of increasing stringency were tried, and the phosphorescence count rates at room temperature were recorded after each wash, both immediately (i.e. about 2 minutes after the wash) and after the phosphorescence had died down to an apparently

constant level (after several hours). Results are given in Table 1: all washes consisted of a linear rise at 5°C/s, with no pause at the maximum temperature.

Table 1: Effect of different washes

Max temp of wash/°C	Immediate intensity/cps	Delayed intensity/cps
125	1000	300 ± 20
175	>250: off scale	15 ± 5
225	215	0 ± 2
225 (second wash)	30	0 ± 2

(All count rates have dark count subtracted. Immediate intensity decays very rapidly, so errors are not estimated.)

Three trivial explanations of the phenomenon were rejected:

(i) An increased dark count of the PMT at switch-on (the EHT was switched off during the wash): this could be ruled out because the dark count was monitored by interposing a blanking plate in the beam path.

(ii) An effect similar to spurious TL: the washes were done in high purity nitrogen, and between washes the sample was kept in vacuum.

(iii) Thermal lag: it can be seen from the time scale of the diagrams that the phenomenon lasts too long for this by about two orders of magnitude.

Given that the effect is real, it might be thought that transfer of electrons from the high temperature peaks to the low temperature peaks was happening, especially as the time dependence of the phosphorescence is similar to that of thermal phoshorescence from the low tempertature peaks (Fig 1). However, no corresponding repopulation of either the 90°C or 130°C peaks is observed. This could be explained if these peaks were thermally quenched in TL: however, a comparison of peak area with rate of thermal phophorescence at room temperature from a given dose showed that if any thermal quenching did take place, the effect was too small by a factor of at least 20 to account for postwash phosphorescence.

Further experiments were made, to find the effect of repeated washes (Fig 2): the signal is partially regenerated by reheating.

The spectrum of the phosphorescence was taken, using a series of edge cut filters in the beam path, and a subtraction technique. For comparison a similar spectrum was obtained for thermal phosphorescence from the low temperature traps. There is some correlation between the two spectra, but the emission peak at

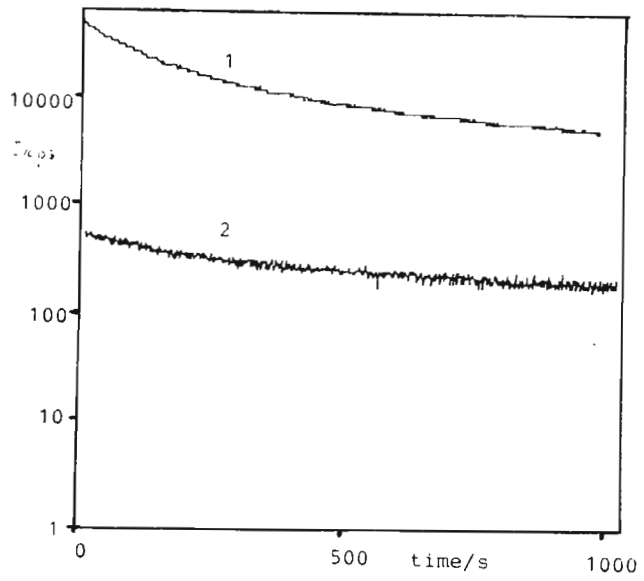

Figure 1: Comparison of post wash phosphorescence with thermal phosphorescence from the low temperature peaks. Dose was 5200 Gy, wash was to 155°C at 5°C/s.
1. Thermal phosphorescence.
2. Post wash phosphorescence.

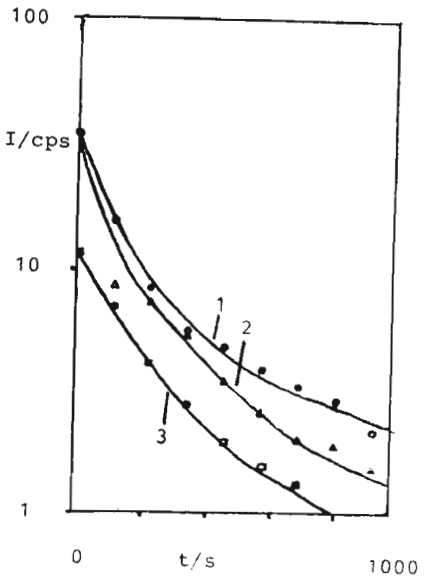

Figure 2: Effect of repeated washes. A sample was dosed with about 70 Gy and left until thermal phosphorescence has ceased, then repeatedly washed to 100°C. The dark count of the PMT is subtracted.

480nm in the thermal phosphorescence does not appear in the post wash spectrum, and the proportions of the emission peaks at 370, 450 and 580nm seem to differ.

A possible model for the phosphorescence is based on the idea of a reservoir trap to which some of the electrons from the deep TL traps are transferred during the wash. Because of a very low frequency factor escape of these electrons from the reservoir traps, they are not evicted during the wash, nor do they give rise to a low temperature TL peak. It is thought that a localised transition state involving the deep trap, the reservoir trap and the luminescent centre is involved (Halperin and Braner 1960), connecting the phenomenon with Templer's localised transition model for anomalous fading. Both models will be discussed in forthcoming articles by Templer and myself.

Post wash buildup

This effect was first discussed by Petridou et al (Petridou et al, 1978), for lithium fluoride, although they have observed it in other materials since. After thermally washing an irradiated sample, a TL peak at a temperature lower than the maximum washing temperature is observed, its peak area building up with time after wash. The current explanation from the same group is in terms of migrating radiation defects forming triplets with electron/hole pairs (Kitis et al.,1985).

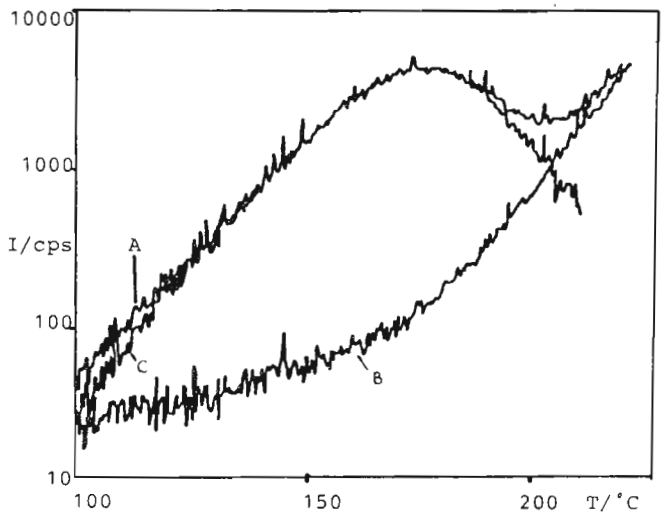

Figure 3: Post wash buildup in Zircon: 5200 Gy, 25.5 hrs after washing to 295°C. Glowed out at 5°C/s. Curve A is the delayed glow curve, B a prompt glow curve, and C the result of subtracting the two.

In the case of zircon, buildup of a peak at 172°C (for a heating rate of 5 °C/s) has been observed in the sample 210R2, which was one of the samples used for the experiments on post wash luminescence. This does not correspond to any TL peak normally observed.

In order to eliminate the possibility of spurious TL, the samples were stored under vacuum, and glowed out in high purity nitrogen. Glow curves were stored on a 4096 channel MCS so that subtraction of the prompt glow curves could be used to reveal the buildup peak (Fig 3).

Two rates of heating (1.05 and 5°C/s) were used for glowing out the samples to allow determination of E and s values by peak shift, and two pause times were used (25.5 and 94.65 h). The E and s values were also determined by the initial rise method. Results are summarised in Table 2. The calculations were based on first order TL peaks, which is not necessarily correct: nevertheless it is noticeable that

(i) E values are very low, in the range 0.28eV to 0.52ev.

(ii) E values determined by peak shift are in all cases lower than those derived from initial rise.

(iii) s values are down by about six orders of magnitude on the values associated with normal TL peaks.

No explanation of (ii) is offered, but it may be noted that low E and s values are not inconsistent with the defect diffusion model.

Table 2

Delay/hrs	β / (°C/S)	T peak /°C	E_{ir} /eV	E_{ps}
0	any	no peak	n/a	n/a
25.5	5	172	0.443±0.013	0.292±0.10
94.65	1.05	109	0.519±0.022	0.282±0.012
94.65	5	174	0.350±0.04	0.352±0.018
25.5	1.05	117	0.380±0.017	

Abbreviations: β = heating rate
ir = initial rise
ps = peak shift

References

Halperin, A. and Braner A.A. (1960) Evaluation of thermal activation energes from glow curves. Phys. Rev., 117,408.

Kitis, G., Hasan, F. and Charalambous, S. (1985). Regenerated thermoluminescence - some new data, Nucl. Tracks, 10 (4-6), 565-570.

Petridou, Ch., Christodoulides, C. and Charalambous, S. (1978). Non-radiation induced thermoluminescence in pre-irradiated LiF (TLD-100), Nucl. Instrum. Meth., 150, 247-252.

Templer, R.H. (1985), The removal of anomalous fading in zircon. Nucl. Tracks, 10 (4-6), 531-537.

P.I. Reviewer's Comments (Peter Townsend)

It seems a pity that the term thermal wash has come into common usage since thermal anneal is more appropriate. *(Ed; I agree)*

Based on spectral results we have obtained in our laboratory (see below), we have reached a similar conclusion concerning the possibility of a diffusion stage the zircon TL signal change. In fact this process is probably quite common, but often ignored.

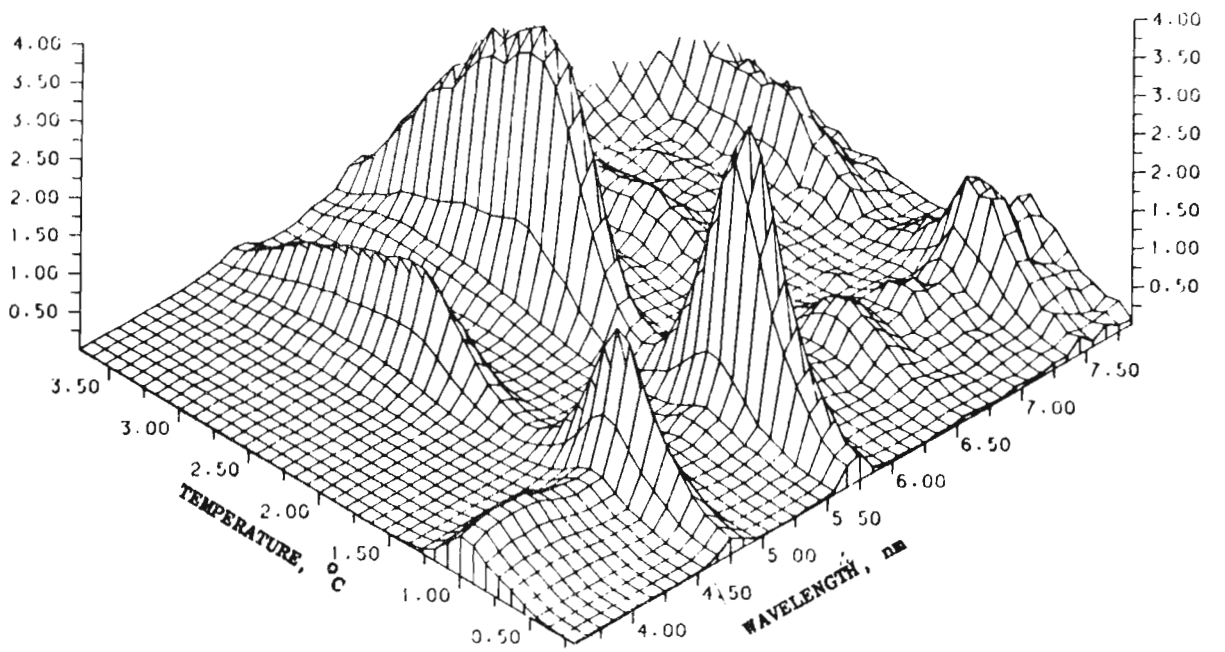

TL spectrum of a green zircon taken at 20°C per min. Low T blue peak (400nm) is from a different impurity from the others and fades faster, bleaches at a different rate and is sample dependent. Current suggestions include evidence for a regeneration of the 100°C/575nm feature from the decay, or movement of other traps. The peak appears even after 30 days storage. Subtle changes occur in the higher temperature peak spectra on storage. A paper is planned which will show more of these details.

J. Chee, T. Hedde, Y. Kirsh, H.L. Oczkowski, J.A. Strain and P.D. Townsend.

Paleographical and stratigraphical inferences from TL properties of Saalian & Weichselian loess of NW Europe

Sanda Balescu*
Christian Dupuis and Yves Quinif**

*Aspirant FNRS
Laboratories Associés de Géologie, Pétrologie et Géochronologie
Université Libre de Bruxelles
50 av. F.-D. Roosevelt
1050 Bruxelles, Belgium

**Laboratoire de Minéralogie
Faculté Polytechnique de Mons (FAPOM)
9 rue du Houdain
Mons, Belgium

Introduction

In this paper we report on stratigraphical and paleogeographical inferences from a comparative TL investigation of Saalian and Weichselian loess of Northwestern Europe. The aim of the research, carried out at the Laboratory of Mineralogy of the FAPOM in Mons, Belgium, is to study the stratigraphical and spatial variations of the loess TL characteristics. Evidence of such variations would provide new promising means for loess identification, stratigraphical correlation and paleographical reconstitution.

Materials and methods

We have selected several reference loess sequences under stratigraphical control, from northern Belgium to Normandy (France), as shown in figure 1. We confined ourselves to the analysis of truly aeolian loessic deposits as they can be assumed to be optically bleached under sunlight during aeolian transportation, prior to their deposition (Wintle and Huntley, 1982). The different loess sections investigated are schematically presented in figure 2. On one hand, we sampled the Late Glacial

FIG 1

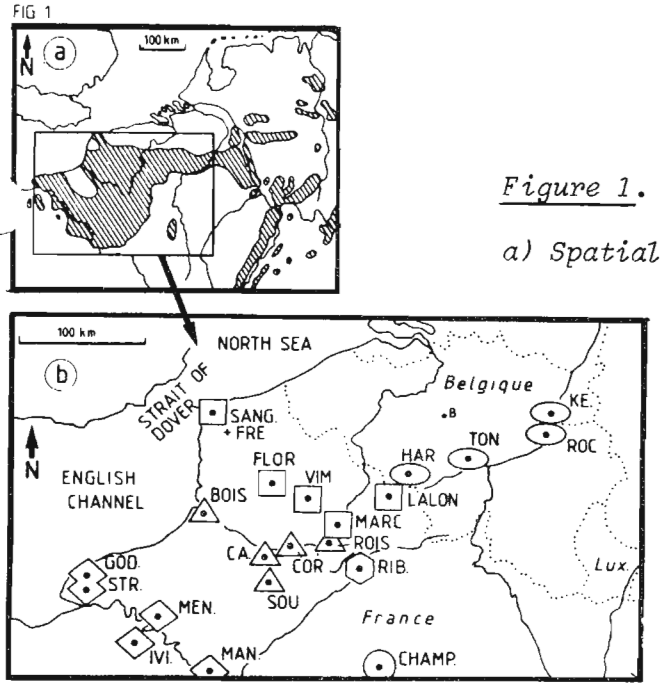

Figure 1.

a) Spatial distribution of NW European loesses.

b) Locality map.

References:

TON (Paepe and Vanhoornem, 1967)
HAR KE ROC (Haesaerts et al., 1981)
CA, SANG (Balescu and Haesaerts, 1984)
FLOR (Tuffreau, 1975)
VIM MARC LALON (Sommé and Tuffreau, 1976)
BOIS (Devismes et al., 1977)
STR GOD MEN (Lautridou, 1968)
IVI (Dewolf Y. et al., 1981)
MAN (Vazart, 1983).

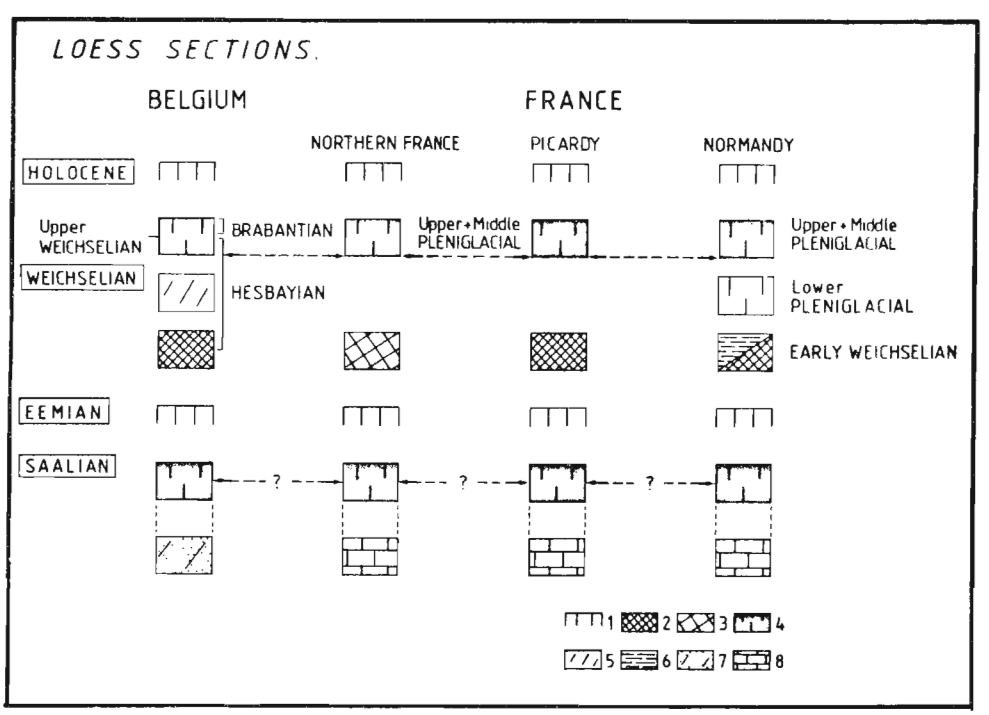

Figure 2. Loess sections.
Key 1. illuviated soil (brown forest soil); 2. grey loam (steppe soil); 3. grey hydromorphic loam; 4. loess; 5. loams; 6. clayey loam; 7. sandy substrate; 8. chalky substrate.

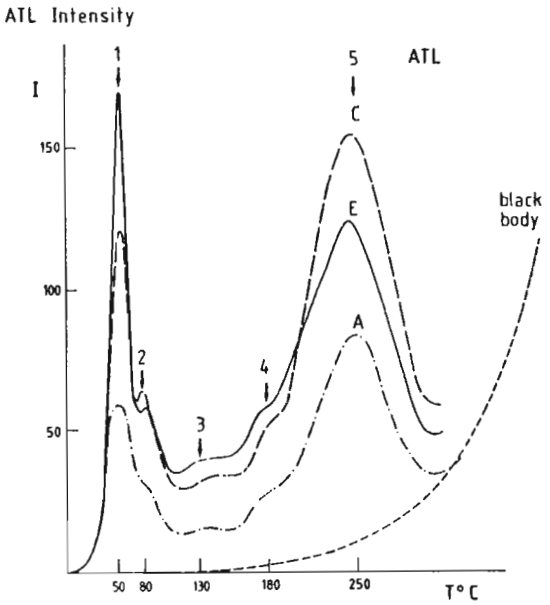

Figure 3a. Examples of quartz ATL glow curves, corresponding to types A, C and E shown in figure 3b.

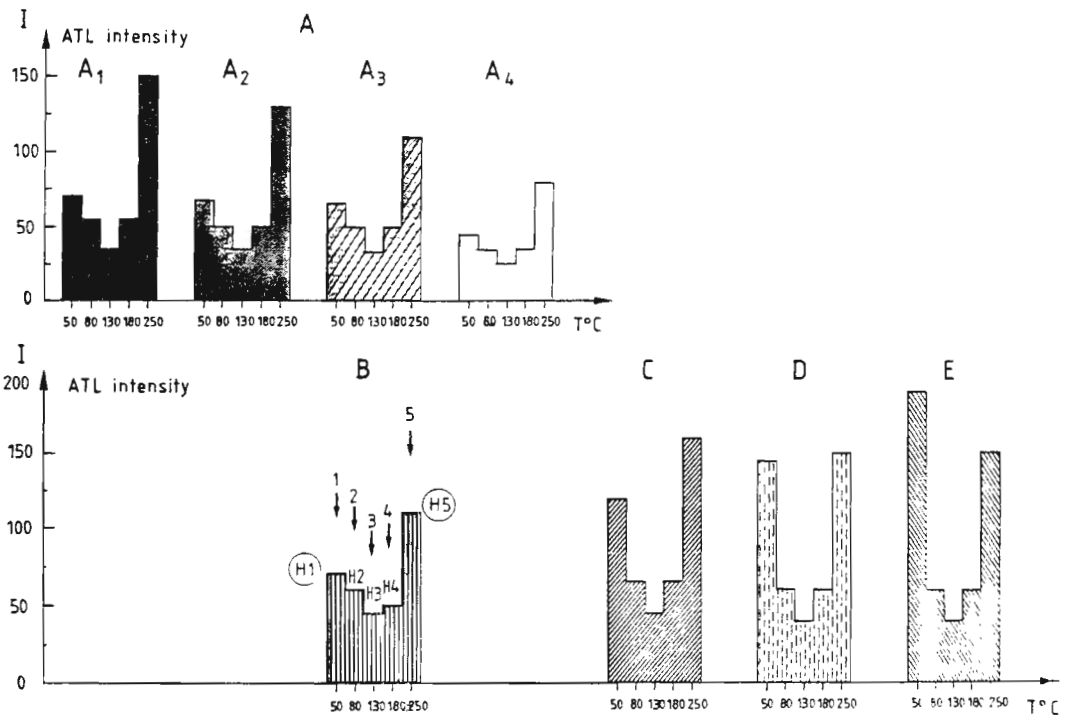

Figure 3b. Quartz ATL typology of NW European loesses from samples which have been γ irradiated for 12 h after being bleached by a 24 h exposure to the sunlamp. Schematic representation of ATL glow curves where mean peak intensities (related to the height of the peak, in arbitrary units) are plotted as a function of temperature (°C).

Representation of five distinct types of ATL glow curves, A,B,C,D and E according to variations in absolute and relative intensities of their first (50°C) and fifth (250°C) peaks (H1 and H5).

Mean intensities of the peaks were calculated using the results from several samples collected in different loessic deposits characterized by the same type of curve.

Weichselian loess on top of which is developed the surface soil, a remnant of the Holocene pedogenesis. On the other hand, we collected samples from the Saalian loess which are systematically underlying the Eemian illuviated soil.

We concentrated on the analysis of the pure detrital quartz grains of the 40-50 μm grain size fraction, using both artifical (ATL) and natural (NTL) TL glow curves. The quartz samples were irradiated for 12 hours with a Co60 γ source after being UV bleached by a 24 h exposure to a sunlamp. We refer to the papers of Charlet (1969) and Baleine (1973) for further technical details.

Results and discussion

The ATL curves from samples of both Weichselian and Saalian loess comprise five peaks lying between 50°C and 250°C and occuring, in all curves, at the same temperature, as shown in fig 3a (1 to 5). Variations in absolute and relative intensities of the lowest and the highest temperature peaks (50°C and 250°C), lead us to define five different types of curves (A,B,C,D and E), corresponding to distinct curve shapes, as shown in fig 3b. One can distinguish asymetrical curves with a dominant fifth peak (types A,B,C) or a dominant first peak (type E) and symmetric curves (type D).

The ATL glow curves were found to be similar within the whole individual loessic deposit, and thus allows us to use the ATL signal as a new sedimentological marker for loess identification. The finding of a variety of types demonstrates the existence of distinct quartz assemblages within northwestern European loess.

The NTL glow curve, obtained from the same quartz samples, comprises a double peaked glow curved. The two TL peaks occur at the same temperature as the two highest temperature peaks of the ATL glow curve. In figure 4a the intensity of the highest temperature peak of the NTL glow curve has been plotted versus intensity of the corresponding artifical peak. As is clear from the figure, the NTL intensity sucessfully discriminates between Saalian (unshaded symbols) and Weichselian (shaded symbols) loess. Indeed, all Weichselian loess show systematic and significantly lower NTL intensities (illustrated in the schematic insets to figure 4a). However, the NTL signal does not allow any further stratigraphical discrimination among Saalian loess since it has reached saturation (see figure 4b).

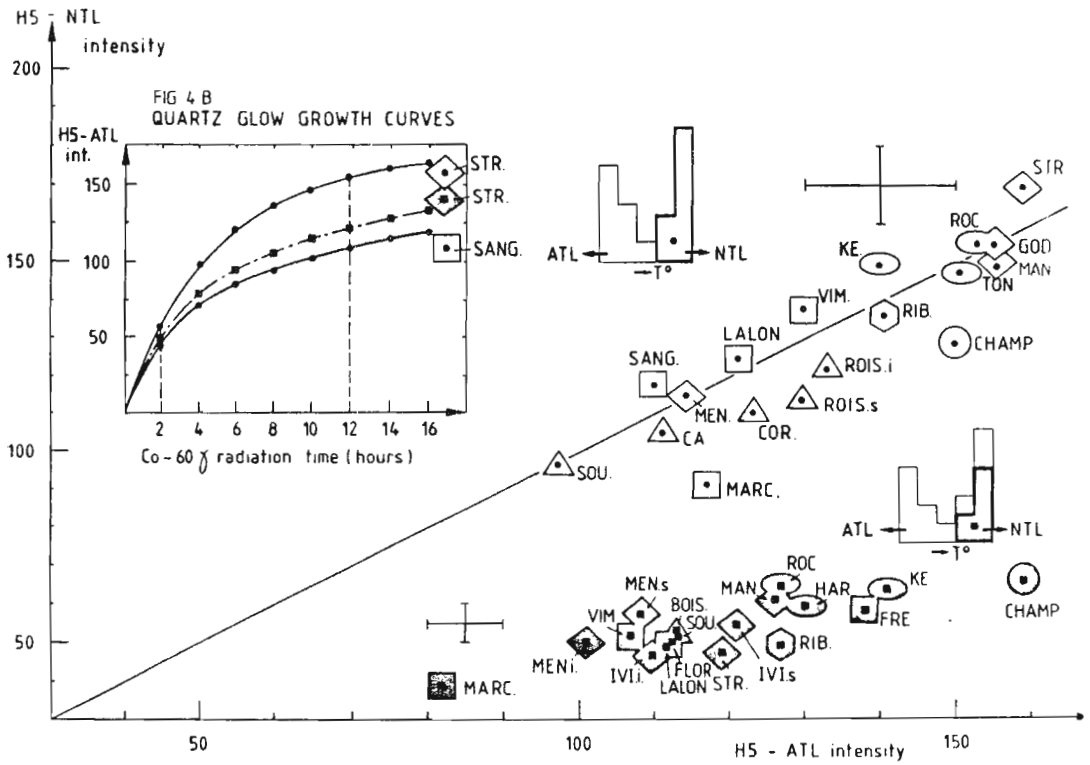

Figure 4. a) Quartz NTL-ATL diagram. Intensity of the highest temperature natural glow curve peak (250°C) versus intensity of the corresponding artifical peak; samples have been exposed for 24 h to uv radiation before being γ irradiated for 12 h (intensity in arbitrary units).

b) Quartz second growth glow curves at 250°C glow curve temperature, after samples have been uv bleached by sunlamp for 24 h (TL in arbitrary units versus γ irradiation time in hours).

A simultaneous use of both ATL and NTL glow curves leads us to define distinct Weichselian and Saalian loessic provinces and to establish paleographical maps, as shown in figure 5a. The inter-province heterogeneity of the quartzose material could involve a diversity in the sediment provenance and source areas of the northwestern European loess. A comparison of the Saalian and Weichselian loessic provinces reveals either a similarity or a difference in their quartz ATL characteristics, reflecting either a constancy or a time change in their sediment provenance.

The results of heavy mineral analysis have supported our TL investigation and allows definition of specific Weichselian and Saalian loessic provinces on the basis of their green hornblende and garnet content, as shown in figure 5b. Information gathered by both heavy material and TL analysis are generally in good agreement. There are, however, some significant discordances, as can be seen by comparing the respective paleogeographical maps (figs. 5a and 5b). This makes both methods complementary. Consequently, a concurrent use of the loess NTL properties - for time control - together with their ATL characteristics and heavy mineral content - for better paleogeographical control - provides a new stratigraphical marker for loess.

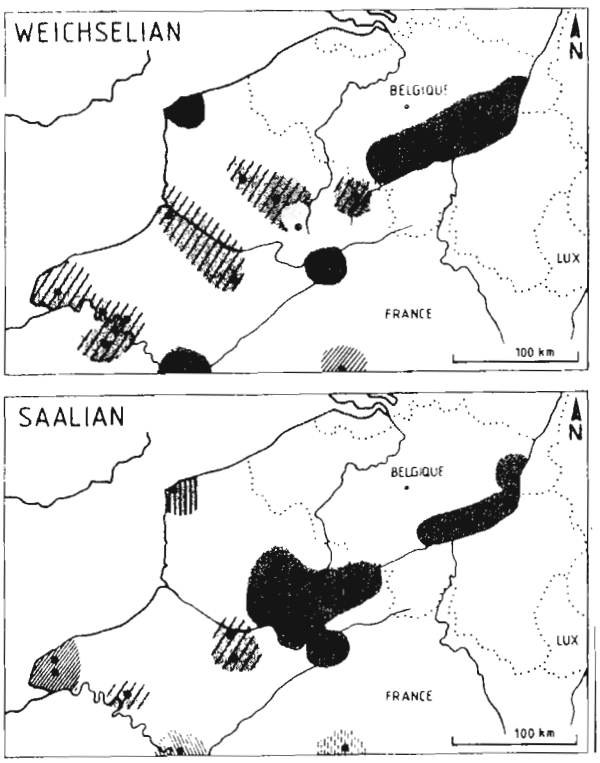

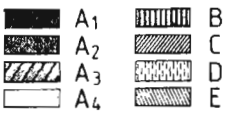

Figure 5a. Spatial distribution of ATL quartz assemblages within Saalian and Weichselian loesses. Quartz ATL assemblages referring to the quartz ATL typology defined in figure 3

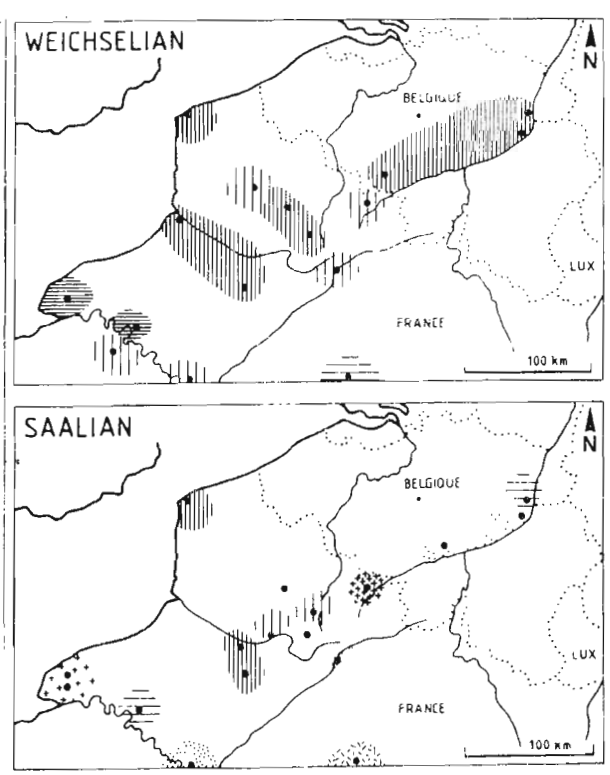

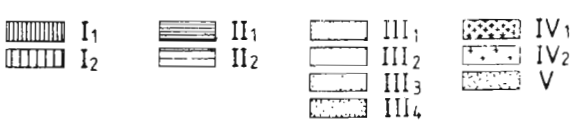

Figure 5b. Spatial distribution of green hornblende and garnet associations within Saalian and Weichselian loesses. Average green hornblende (GH) and garnet (G) content (in %) estimated on total count of 300 transparent heavy mineral grains per sample: H ≈ 20%, M ≈ 10%, L ≈ 5%, VL ≈ 1-2%, A ≈ 0%.

$$-I_{1-2} = \underline{H.(GH)} + M\text{-}L.(G);$$

$$-II_{1-2} = \underline{M.(GH)} + VL.(G);$$

$$-III_{1-2-3-4} = \underline{L\text{-}VL.(GH)} + L\text{-}VL.(G);$$

$$-IV_{1-2} = L\text{-}VL.(GH) + \underline{A.(G)};$$

$$-V = \underline{A.(GH)} + VL.(G).$$

Conclusion

Our results clearly demonstrate the important potential of the quartz TL method for identification, stratigraphical correlation and relative age determination of these isolated and discontinuous aeolian deposits. Furthermore, the remarkable stratigraphical and spatial coherence of these TL results show great promise for the identification of source areas of these loesses and to establish a reference loess stratigraphical scheme for NW Europe.

References

Baleine, O., Charlet, J.M. and Dupuis, C. (1973) Les techniques utilisées pour l'étude de la thermoluminescence au laboratoire de minéralogie de la F.P.Ms; 10 années d'expérience. Ann. Scientifiques du Department des Mines-Géologie, 1, 34-48.

Balescu, S. and Haesaerts, P. (1984) The Sangatte raised beach and the age of the opening of the Strait of Dover. Geol. en Mijnbouw, 63, 355-362.

Charlet, J.M. (1969) La thermoluminescence des roches quartzofeldspathiques. Applications á l'étude des séries sédimentaires détritiques; intérét dans la datation des granities Bull. B.R.G.M., 2e série, 2, 51-97, and 3, 11-60.

Devismes, R., Dupuis, C., Haesaerts P. and de Heinzelin, J. (1977) Fouilles de 1975 á la carriére est du chemin des Salines, Boismont, Somme, France. Cahiers Archéologiques de Picardie, 4, 31-42.

Dewolf, Y., Helluin, M., Lautridou, J.P. and Vazart, M. (1981) Les loess d'Iville (Eure). Faciés régional de transition entre deux provinces loessiques majeures du Bassin de Paris . Bull. A.F.E.Q., 3-4, 159-172.

Haesaerts, P., Juvigne, E., Kuyl, O., Mucher, H. and Roebroeks, W. (1981) Compte rendu de l'excursion du 13 juin 1981, en Hesbaye et au Limbourg néer landais, consacrée á la chronostratigraphie des loess du Pléistocène supérieur. Annales de la Société Géologique de Belgique, 104, 223-240.

Lautridou, J.P. (1968) Les loess de Saint Romain et de Mesnil-Esnard. Bull. Centre Géom., 2, 55.

Paepe, R., Vanhoorne, R. (1967) The stratigraphy and paleobotany of the Late Pleistocene in Belgium. Mém. Expl. Cartes Géol. et Min. Belg., 8.

Somme, J., Tuffreau, A. (1976) Vimy (Pas-de-Calais): 191-194; Marcoing (Nord France): 205-209; La Longueville (Nord France): 214-217. Livret guide Préhistoriques et Protohistoriques.

Tuffreau, A. (1975) Acheuléen dans les limons anciens de Floringhem (Pas-de-Calais). Septentrion, 5, 37-39.

Vazart, M. (1983) Paléodynamiques weichséliennes des provinces normandes, vexinienne et séquanienne (Analyse micrographique). Travaux du laboratoire de géographie physique, 11, 81p.

Wintle, A.G. and Huntley, D.J. (1982) Thermoluminescence dating of sediments. Quaternary Science Reviews, V. 1, 31-53.

P.R. Reviewers Comments (A.M.D. Gemmell)

The use of NTL and ATL curves to distinguish detrital sediments of different provenances has been known for several years (Charlet, 1971). The present study takes this approach a stage further by applying the technique to loessic sediments, and using it not only to distinguish palaeographic provinces, but as a tool for stratigraphic correlation.

In respect of the latter use, a number of questions arise. As no bleaching curves are presented, overbleaching may have occurred. Wintle (1985) has suggested that dose-dependent sensitivity changes may occur when a sample is exposed to light, but whether such dose dependent changes would survive significant changes in the samples in the present study might provide an answer to this question.

Closer examination of figure 4a shows clearly that ATL characteristics fail to separate Saalian and Weichselian sediments, and it is the NTL which is the discriminating factor. As the NTL of the Saalian loesses has reached saturation level (Balescu, Dupuis and Quinif, this issue), then the technique is unlikely to be useful for the stratigraphic correlation of older deposits.

If the various quartz assemblages identified in this study represent differences in the composition of loess due to changes in wind direction, some of the sediment may not have been transported far enough from its source for complete bleaching to have taken place prior to deposition. if the sources can be identified, and assuming that the loesses are securely dated by other techniques, than the significance of transport distance as a possible influence on the TL-age of loessic sediments can be investigated.

References

Balescu, S., Dupuis, C. and Quinif, Y. (This volume). Paleogeographical and stratigraphical inferences from thermoluminescence properties of Saalian and Weichselian loesses of northwestern Europe.

Charlet, J.M. (1971) Thermoluminescence of detrital rocks used in paleogeographical problems. Modern Geology, 2, 265-274.

Wintle, A.G. (1985) Sensitization of TL signal by exposure to light. Ancient TL, 3 (3), 16-21.

The Editor is grateful to Mrs. W. Musgrave (wordprocessing) and Mr. S. Clogg (production) for assistance in the preparation of this issue of Ancient TL.

Bibliography

Akhter, S.H., Bhattacharya, A.K., Sen Gupta, D.K. and Kaul, I.K. (1985) Significance of thermoluminescence of the crystalline limestones of Jabar (Purulia District, West Bengal, India). Nucl. Tracks Radiat. Meas., 10, 193-199.

Azorin, J.N., Gutierrez, A.C. and Martinez, C.G.A. (1985) Determination of activation energies and frequency factors of dysprosium-activated calcium sulfate thermoluminescent dosimeters. Radiation Effects, 84, 263-280.

Amin, Y.M. and Durrani, S.A. (1985) A spectral study of TL from natural zircons. Nucl. Tracks Radiat. Meas., 10, 55-60.

Bahadur, H. and Parshad, R. (1985) On the purple and violet light emissions in thermoluminescing quartz. Phys. Status Solidii, 91, 191-197.

Bluszcz, A. and Pazdur, M.F. (1985) Proposal for the quotation of TL dates for sediments. Przeglad Geologiczny, 385(5), 277-281.

Bull, R.K. and Durrani, S.A. (1985) The thermal stability of thermoluminescence in chondritic meteorites. Nucl. Tracks Radiat. Meas., 10, 169-175.

Butrym, J. and Maruszczak, H. (1984) Thermoluminescence chronology of younger and older loesses. In Lithology and Stratigraphy of Loess and Paleosols, ed. M. Pecsi, 195-199, published by the Geographical Research Institute of the Hungarian Academy of Sciences, Budapest.

Christodoulides, C. (1985) Determination of activation energies by using the widths of peaks of thermoluminescence and thermally stimulated depolarization currents. J. Phys. D, 18, 1501-1510.

Christodoulides, C. (1985) Errors involved in the determination of the activation energies in TL and TSDC by the initial rise method. J. Phys. D, 18, 1665-1671.

David, M. (1985) Thermoluminescence of quartz: Part XII - Effect of neutron irradiation. Indian Journal of Pure and Applied Physics, 23, 267-269.

De, R., Rao, C.N. and Kaul, I.K. (1985) Implications of diagenesis for the TL dating of the oceanic carbonate sediments in the northern Indian Ocean. Nucl. Tracks Radiat. Meas., 10, 185-192.

Goede, A. and Bada, J.L. (1985) Electron spin resonance dating of Quaternary bone material from Tasmanian caves - a comparison with ages determined by aspartic acid raceminzation and C^{14}. Australian J. Earth Sci., 32, 155-162.

Guimon, R.K., Keck, B.D., Weeks, K.S. de Hart, J. and Sears, D.W.G. (1985) Chemical and physical studies of type 3 chondrites IV annealing studies of a type 3.4 ordinary chondrite and the metamorphic history of meteorites. Geochim. et Cosmochim. Acta, 49, 1515-1524.

Hasan, F.A. (1985) Thermoluminescence as a function of dose in natural calcium fluoride: a proposed mathematical model. Nucl. Instrum. Methods Phys. Res., Sect B12, 175-180.

Herforth, L., Huebner, K. and Stolz, W. (1985) Thermoluminescence in dosimetry and geosciences. Ann. Phys. (Leipzig), 42 461-470. (in German)

Kriegseis, W. and Scharmann, A. (1985) Determination of free quartz surfaces in coal dust. Ann. Occup. Hyg., 29 91-99.

Levy, P.W. (1985) Recent developments in thermoluminescence kinetics. Nucl. Tracks Radiat. Meas., 10, 21-32.

Li, H.H. (1985) Thermoluminescence properties of calcite from Ertan, Sichuan Province. Kexue Tongbao, 30, 380-383.

Li, H.H. (1985) Formation age of Malan loess dated by thermoluminescene (TL) of quartz. Kexue Tongbao, 30, 1091-1094.

McKeever, S.W.S., Rhodes, J.F., Mathur, V.K., Chen, R., Brown, M.D. and Bull, R.K. (1985) Numerical solutions to the rate equations governing the simultaneous release of electrons and holes during thermoluminescence and isothermal decay. Physical Review B, 32, 3835-3843.

Mejdahl, V. (1985) Thermoluminescene dating based on feldspars. Nucl. Tracks Radiat. Meas., 10, 133-136.

Miallier, D., Fain, J. and Sanzelle, S. (1985) Single-quartz-grain thermoluminescence dating : an approach for complex materials. Nucl. Tracks Radiat. Meas., 10,163-168.

Nagatomo, T. (1984) Themoluminescent dating of earthenwares and other related materials. Kobunkazai no Kagaku, 29, 83-93. (in Japanese)

Nambi, K.S.V. (1985) Scope of electron spin resonance in thermally stimulated luminescence studies and in chronological applications. Nucl. Tracks Radiat. Meas., 10, 113-131.

Pei, J.X., Xu, X.H. and Ki, J.L. (1985) Thermoluninescence dating of calcite in the gouge of F-20 fault at Ertan Dam site. Scientia Sinica (Series B), 28, 1000-1007.

Poupeau, G. (1983) The archaeological dating by thermoluminescence: a review report CBPF-NF-003/83, 57 pages. (in French)

Sankaran, A.V., Nambi, K.S.V. and Sunta (1985) Thermoluminescence of laterites. Nucl. Tracks Radiat. Meas., 10, 177-183.

Singhvi, A.K. and Mejdahl, V. (1985) Thermoluminescence dating of sediments. Nucl. Tracks Radiat. Meas., 10, 137-161.

Singhvi, A.K., Nambi, K.S.V., Durrani, S.A., Sunta, C.M. and Mejdahl, V. (1985) editors of Theory and Practice of Thermally Stimulated Luminescence and related phenomena - 1984 Ahmedabad. Nucl. Tracks Radiat. Meas., 10, 289 pages.

Wintle, A.G. (1985) Letter to the editor on the analysis of complex thermoluminescent spectra. Journal of luminescence, 33, 333-334.

Wintle, A.G. and Catt, J.A. (1985) Thermoluminescence dating of Dimlington Stadial deposits in eastern England. Boreas, 14, 231-234.

APPLICATION DEADLINE EXTENDED

UNIVERSITY OF WASHINGTON

Thermoluminescence Dating Laboratory

The UNIVERSITY OF WASHINGTON seeks a research associate for its newly established thermoluminescent dating facility, being developed jointly between the Departments of Materials Science and Engineering and Anthropology. Duties of this research associate will include developing the facility, teaching and conducting research in TL dating techniques, and managing the overall operation of the laboratory. Current National Science Foundation funding is secure through 1988; however, the appointee is expected to develop additional outside funding by the second year of appointment. Candidates should have a Ph.D. and a minimum of 2 years experience in TL dating. Interested parties should address a request for a detailed description of the position, along with a current resume and statement of interest to: Dr. T.G. Stoebe, College of Engineering, FH-10, University of Washington, Seattle, WA 98195.

Erratum

"A correction procedure for ambient activation in pre-dose dating"

Sutton and Kornmeier

Volume 3, No. 3

Three delta (Δ) symbols were omitted.

1. p.2: The sentence following equation 3 should read "The difference Δ_T between the original ..."

2. equation 7: $D_n = \frac{\{S_{n,max} - S_o\}}{\{S_{n,max} - S_o^*\}}$ $D_n^* = \frac{D_n^*}{1-\Delta_T(max)}$

3. p.4: The last sentence should read "... and Δ values are determined ..."